Acta Cryst. (1998). D**54**, 610–614

On the Choice of an Optimal Wavelength in Macromolecular Crystallography

Alexei Teplyakov,[a]* Glaucius Oliva[b] and Igor Polikarpov[c]

[a]*EMBL, Hamburg Outstation, DESY, Notkestrasse 85, 22603 Hamburg, Germany,* [b]*IFSC/USP, CP 369, Sao Carlos, SP, Brazil, and* [c]*LNLS, CP 6192, CEP 13081-970, Campinas, SP, Brazil. E-mail: alex@embl-hamburg.de*

(*Received 28 August 1997; accepted 24 December 1997*)

Abstract

Potential benefits of using short X-ray wavelengths for protein crystal data collection arise from a reduction in absorption errors and a decrease in radiation damage of a sample. On the other hand, at longer wavelengths one may benefit from an increase in scattering efficiency of a crystal and an increase in intensity of an incident beam at a given synchrotron beamline. For small and frozen crystals the negative effects of absorption and radiation damage would be minimized which may shift the balance of interests towards the use of longer wavelengths. Experiments carried out at EMBL beamlines at DESY (Hamburg) show an advantage of using wavelengths longer than 1 Å for data collection from crystals of up to 0.5 mm.

1. Introduction

Various factors which determine the choice of an optimal X-ray wavelength in macromolecular crystallography have been considered in detail by Helliwell (1992, 1993, 1997). Potential benefits of using very short (0.5 Å) and ultra-short (0.3 Å) wavelengths are the increased sample lifetime and reduced absorption. However, most of available sources of synchrotron radiation provide relatively low fluxes in the high energy range. On the other hand, the use of longer wavelengths enhances scattering efficiency and may be particularly advantageous for small and frozen crystals. Unfortunately, there are very few experimental studies which might help to define relations between all these parameters.

Gonzalez *et al.* (1994) have compared the quality of the data and the background level in the diffraction patterns collected on the SRS (Daresbury) wiggler station 9.5 at 0.92 and 0.55 Å. The sample was a lysozyme tetragonal crystal of a size of 0.3–0.5 mm. The results indicated no improvement in the signal-to-background ratio at very short wavelengths. The $R_{\rm merge}$ for the 0.92 Å data was better than that of 0.55 Å in all resolution shells in spite of the 7.5 times shorter exposures.

We have designed and performed a series of experiments to compare the quality of the data collected from frozen protein crystals at different wavelengths in the range 0.8–1.5 Å. These studies show an advantage of using wavelengths longer than 1 Å for data collection from crystals of up to 0.5 mm.

2. Theory

The choice of an optimal wavelength for data collection is important to compromise between the flux of synchrotron radiation, the scattering efficiency of the protein crystal, and the absorption effects. The integrated X-ray intensity is a function of the wavelength λ and the dimension of the crystal t,

$$I \propto \lambda^2 t^3 \exp(-\mu t)$$

where μ is the absorption coefficient which is approximately proportional to λ^3. As the wavelength increases, the scattering efficiency of the crystal also increases as well as absorption becomes more pronounced. The theoretical curves for a given crystal size are shown in Fig. 1. The optimal wavelength λ_o at which the function reaches its maximum is

$$\lambda_o(\text{Å}) \simeq [3/t(\text{mm})]^{1/3}.$$

It is implied that there is no significant radiation damage of a sample and no additional absorption by the capillary and solution around the crystal which is true for frozen crystals mounted in cryo loops.

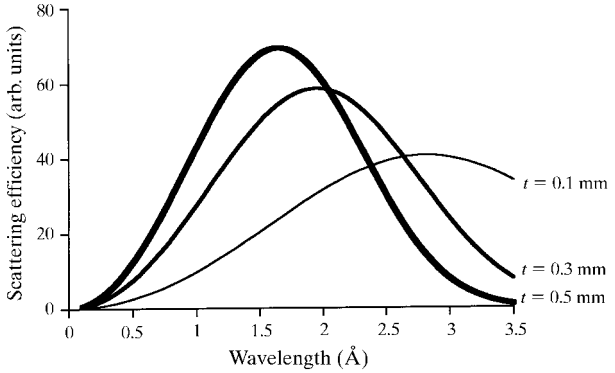

Fig. 1. Scattering efficiency of the protein crystal of thickness t as a function of the wavelength. To be in the same scale, the curves are normalized on the crystal cross section t^2.

ISSN 0907-4449

Table 1. *Data statistics for experiment No. 1 on the wiggler beamline BW7A*

Crystal size was 0.4 × 0.4 × 0.2 mm. $T_{max}/T_{min} = \exp[\mu(t_{max} - t_{min})]$ where t_{max} and t_{min} are the maximum and minimum paths through the crystal. Mean intensity and background values are obtained by averaging, respectively, over the whole image and over the high-resolution background region (*i.e.* excluding diffraction spots). Redundancy is given for reflections measured more than once.

Wavelength (Å)	0.8	1.0	1.54
Absorption coefficient μ (mm^{-1})	0.15	0.30	1.10
T_{max}/T_{min}	1.06	1.13	1.55
Distance (mm)	275	215	125
Resolution range (Å)	17–2.6	17–2.6	17–2.6
Exposure/image at 70 mA (s)	90	90	90
Mean intensity per pixel	330	550	870
Background level per pixel	260	400	520
Number of reflections			
Measured	27945	27800	26641
Unique	14570	15303	15721
Unique measured >1 time	8936	9103	8693
Redundancy	2.5	2.4	2.3
Reflections with $I > 3\sigma$ (%)			
17.0–2.60 Å	84.1	85.7	86.9
17.0–6.90 Å	98.8	99.0	98.9
2.64–2.60 Å	61.0	63.4	68.7
$\langle I \rangle / \langle \sigma \rangle$			
17.0–2.60 Å	15.3	16.4	15.3
2.64–2.60 Å	3.6	4.4	5.4
R_{merge} for all reflections (%)			
17.0–2.60 Å	4.9	4.4	4.5
17.0–6.90 Å	2.2	2.0	2.1
2.64–2.60 Å	22.9	17.9	14.0
R_{merge} for reflections $I > 5\sigma$ (%)	3.6	3.5	4.0
R factor to 0.8 Å data (%)	0.0	5.4	5.8
B factor relative to 0.8 Å data	0.0	0.7	−0.1

Another factor which influences the choice of an optimal wavelength is the spectral distribution of a given synchrotron beamline which depends on the synchrotron source (energy and magnetic field), type of the insertion device (bending magnet or wiggler) and optical elements of the beamline. The critical wavelength λ_c roughly corresponds to the maximum of spectral density at the source and lies in the range 0.8–3.0 Å for most of the second-generation synchrotrons (Helliwell, 1992). X-ray absorption in Be windows and air defines the long-wavelength edge of the spectrum at about $\lambda = 3$ Å. Mirrors remove hard X-rays with $\lambda < 0.5$ Å. With respect to bending magnets, wigglers expand the spectral range to shorter wavelengths.

Taken together, these factors determine the choice of an optimal wavelength for an X-ray diffraction experiment at a given beamline for a given crystal. These considerations suggest using wavelengths of 1 Å and longer for the crystals which are normally used in macromolecular X-ray analysis (Polikarpov *et al.*, 1997).

3. Spectral characteristics of beamlines

X-ray diffraction experiments were carried out at beamlines X31 and BW7A positioned at the DORIS III storage ring of DESY (Hamburg), X31 on a bending magnet, BW7A on a wiggler. The critical wavelength is 0.8 Å on X31 and 0.9 Å on BW7A at 4.5 GeV. Both beamlines are equipped with double-crystal Si(111) monochromators which allow tuning the wavelength. X31 has an Au-coated focusing mirror, BW7A has two Rh-coated mirrors.

To determine the range of wavelengths suitable for data collection, the spectral distribution of these beamlines was measured with an ion chamber positioned after the optical elements and the collimator just in front of the sample. The wavelength was varied in the range 0.6–2.1 Å. The position of the optical bench (on X31) or the position of the monochromator (on BW7A) was optimized for each wavelength. The ion chamber response is proportional to the absorption coefficient (λ^3) and the energy of the X-rays ($1/\lambda$). Therefore, the number of counts of the ion chamber was divided by λ^2 to give the relative number of photons. The spectral distribution of the bending magnet beamline X31 (Fig. 2) has a sharp maximum in the range 0.9–1.2 Å and drops smoothly at longer wavelengths. A similar distribution although shifted to shorter wavelengths is observed for the wiggler beamline BW7A (Fig. 3). Its maximum lies in the range 0.7–0.9 Å.

4. X-ray diffraction experiments

Diffraction experiments at different wavelengths were carried out using crystals of glucosamine 6-phosphate synthase (Obmolova *et al.*, 1994). They belong to the space group $R32$ with cell axes $a = 143.7$, $c = 173.6$ Å, and diffract to about 2 Å resolution. Data were collected close to the diffraction limit of the crystal using one crystal for each series of experiments. To exclude the effects of radiation damage, the crystals were frozen and data were collected at 100 K. Diffraction patterns were recorded with a Mar 180 mm image-plate detector. The image-plate response does not change much in the range

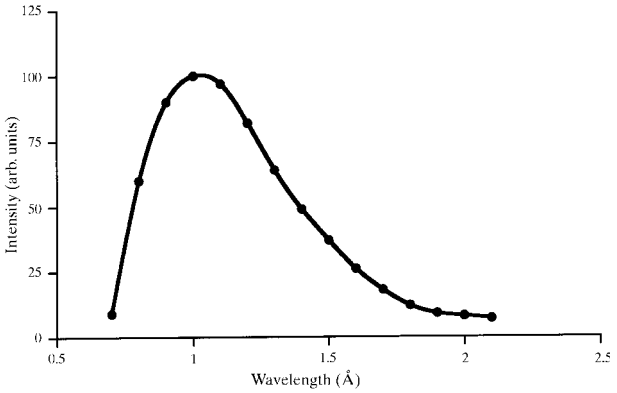

Fig. 2. The spectral distribution of the bending magnet beamline X31. The flux measured by the ion chamber was corrected for the wavelength dependence of the ion-chamber response ($\sim \lambda^2$).

Table 2. *Data statistics for experiment No. 2 on the bending magnet beamline X31*

Crystal size was 0.5 × 0.5 × 0.25 mm. $T_{max}/T_{min} = \exp[\mu(t_{max} - t_{min})]$ where t_{max} and t_{min} are the maximum and minimum paths through the crystal. Mean intensity and background values are obtained by averaging, respectively, over the whole image and over the high-resolution background region (*i.e.* excluding diffraction spots). Redundancy is given for reflections measured more than once.

Wavelength (Å)	0.9	1.1	1.3	1.5
Absorption coefficient μ (mm^{-1})	0.22	0.40	0.66	1.01
T_{max}/T_{min}	1.12	1.22	1.39	1.65
Distance (mm)	220	175	140	117
Resolution range (Å)	18–2.35	18–2.35	18–2.35	18–2.35
Exposure/image at 80 mA (s)	150	150	150	150
Mean intensity per pixel	305	570	425	230
Background level per pixel	190	300	180	80
Number of reflections				
Measured	31775	31348	31524	31396
Unique	18924	18796	19478	19958
Unique measured >1 time	9764	9505	9322	9153
Redundancy	2.3	2.3	2.3	2.2
Reflections with $I > 3\sigma$ (%)				
18.0–2.35 Å	87.6	91.1	89.6	85.5
18.0–6.29 Å	98.7	99.2	99.1	98.9
2.39–2.35 Å	72.8	80.3	73.3	65.3
$\langle I \rangle / \langle \sigma \rangle$				
18.0–2.35 Å	16.9	20.5	20.1	17.9
2.39–2.35 Å	3.9	5.4	5.3	4.2
R_{merge} for all reflections (%)				
18.0–2.35 Å	4.2	3.2	3.2	3.5
18.0–6.29 Å	1.8	1.7	1.9	2.0
2.39–2.35 Å	17.9	13.7	11.8	14.9
R_{merge} for reflections $I > 5\sigma$ (%)	3.2	2.8	2.7	2.8
R factor to 0.9 Å data (%)	0.0	4.2	4.5	5.0
B factor relative to 0.9 Å data	0.0	−0.1	−0.8	−2.1

of wavelengths used in the experiments (Amemiya *et al.*, 1988). The data were processed with *DENZO* and *SCALEPACK* (Otwinowski, 1993). The quality of the data was estimated on the basis of the merging R factor, the number of reflections stronger than 3σ, and the average intensity to sigma ratio.

4.1. *Experiment No. 1*

In the first experiment carried out on the wiggler beamline BW7A, the same oscillation range was measured at three wavelengths, 0.8, 1.0 and 1.54 Å. The short wavelength data were collected first, the long wavelength data were the last. The crystal-to-detector distance was selected so that the resolution limits were the same (17–2.6 Å) for all data sets. The crystal used was of a size of 0.4 × 0.4 × 0.2 mm. The oscillation angle was 1° per image and the total oscillation range was 40° which gave sufficient redundancy of the data. The exposure time was set to be the same at different wavelengths, about 90 s at 70 mA current, by setting the appropriate dose per image. The results are presented in Table 1. The quality of data collected at longer wavelengths is better with respect to the 0.8 Å data in spite of the fourfold decrease in the flux at 1.54 Å (Fig. 3). The difference in quality is particularly pronounced at high resolution. The percentage of reflections with $I > 3\sigma$ increases from 61 to 69% whereas the total number of reflections remains the same, about 1300. The I/σ ratio increases from 3.6 at 0.8 Å to 5.4 at 1.54 Å. The R_{merge} also indicates a significantly better quality (14.0 *versus* 22.9%) of high-resolution data measured at a longer wavelength.

Merging R factors for low-resolution data as well as for strong ($I > 5\sigma$) reflections indicate a somewhat better quality for the 1.0 Å data. We think this is due to different statistics for strong and weak reflections. For strong reflections which dominate at low resolution, the random error is relatively small and the overall statistics are governed by the systematic error due to absorption effects which are more pronounced at longer wavelengths. For weak reflections (= high resolution) the random error dominates the statistics which improves as diffraction becomes stronger, *i.e.* at longer wavelengths.

4.2. *Experiment No. 2*

The second experiment was carried out on the bending magnet beamline X31 at four wavelengths, 0.9, 1.1, 1.3 and 1.5 Å. The crystal size was 0.5 × 0.5 × 0.25 mm. The crystal-to-detector distance was selected so that the resolution limits were the same (18–2.35 Å) for all data sets. Images were collected with an oscillation angle of 0.75°. The total oscillation range was 21° and consisted of two parts of 10.5°. For the first part, the crystal was oriented with its shortest dimension (0.25 mm) along the beam, and for the second part 90° away so that the absorption effects would be maximized.

The exposure time was set to be the same at different wavelengths, about 150 s at 80 mA current. The results are presented in Table 2. As in the previous experiment, data collected at longer wavelengths are of higher quality with respect to the 0.9 Å data. Even data collected at 1.5 Å show better statistics although the number of photons deposited at the crystal is three times less than that at 0.9 Å (Fig. 2). The quality of the 1.1 Å data is superior to the other data in terms of the I/σ ratio, percentage of strong reflections and overall $R_{\rm merge}$. As in the previous experiment, the $R_{\rm merge}$ for high-resolution reflections is better at a longer wavelength (11.8% at 1.3 Å) whereas the $R_{\rm merge}$ for low-resolution data is better at 1.1 Å.

4.3. *Experiment No. 3*

Another experiment on the bending magnet beamline X31 was carried out for a small crystal (0.2 × 0.2 × 0.2 mm) at two wavelengths, 0.9 and 1.3 Å. The oscillation angle was 0.7° per image and the total oscillation range was 21°. Data were collected in the dose mode by setting the number of counts such that the exposure time was twice longer at λ = 0.9 Å as compared to the 1.3 Å data (Table 3). Under these conditions, the mean intensity per pixel appeared to be similar for both data sets. However, the quality of the 1.3 Å data was significantly better in all resolution shells. The $R_{\rm merge}$ improved from 6.9% at 0.9 Å to 4.9% at 1.3 Å, and from 23.9 to 17.6% at high resolution whereas the average I/σ increased by almost 50%.

Table 3. *Data statistics for experiment No. 3 on the bending magnet beamline X31*

Crystal size was 0.2 × 0.2 × 0.2 mm. $T_{\rm max}/T_{\rm min} = \exp[\mu(t_{\rm max} - t_{\rm min})]$ where $t_{\rm max}$ and $t_{\rm min}$ are the maximum and minimum paths through the crystal. Mean intensity and background values are obtained by averaging, respectively, over the whole image and over the high-resolution background region (*i.e.* excluding diffraction spots). Redundancy is given for reflections measured more than once.

Wavelength (Å)	0.9	1.3
Absorption coefficient μ (mm^{-1})	0.22	0.66
$T_{\rm max}/T_{\rm min}$	1.03	1.10
Distance (mm)	220	140
Resolution range (Å)	20–2.35	20–2.35
Exposure/image at 70 mA (s)	420	210
Mean intensity per pixel	240	240
Background level per pixel	150	110
Number of reflections		
Measured	29422	29300
Unique	11224	11356
Unique measured >1 time	10107	10258
Redundancy	2.6	2.6
Reflections with $I > 3\sigma$ (%)		
20.0–2.35 Å	91.1	92.9
20.0–6.31 Å	98.5	98.6
2.39–2.35 Å	79.6	83.2
$\langle I\rangle/\langle\sigma\rangle$		
20.0–2.35 Å	14.9	18.7
2.39–2.35 Å	3.8	5.5
$R_{\rm merge}$ for all reflections (%)		
20.0–2.35 Å	6.9	4.9
20.0–6.31 Å	2.8	2.2
2.39–2.35 Å	23.9	17.6
$R_{\rm merge}$ for reflections $I > 5\sigma$ (%)	4.2	3.6
R factor to 0.9 Å data (%)	0.0	6.4
B factor relative to 0.9 Å data	0.0	0.4

5. Conclusions

In accordance with theoretical considerations, experiments carried out at the synchrotron beamlines using frozen protein crystals have shown that the higher quality of the data can be achieved by using the wavelengths of 1.1–1.3 Å or even 1.5 Å as compared with 0.8–0.9 Å provided other conditions are similar. In terms of time, the data of equal quality can be collected faster at a longer wavelength. The use of λ ≥ 1.1 Å is particularly advantageous for small (0.2 mm) crystals due to insignificant absorption. Even for the crystals as large as 0.4–0.5 mm the gain from the enhanced scattering efficiency surpasses the negative effect of increased absorption.

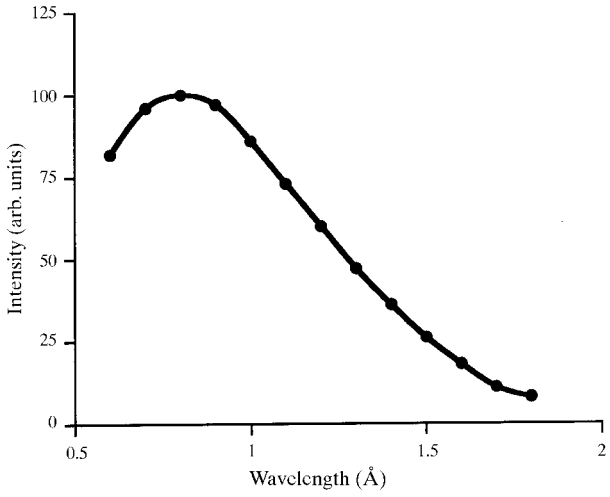

Fig. 3. The spectral distribution of the wiggler beamline BW7A. The flux measured by the ion chamber was corrected for the wavelength dependence of the ion-chamber response ($\sim \lambda^2$).

These experiments show that the optimal wavelength may be slightly different for high- and low-resolution data. In most cases it is the high-resolution shell which determines the overall quality of the data whereas the statistics for low-resolution data are always much better regardless of the wavelength. Therefore, the choice of the optimal wavelength would be oriented towards higher quality at high resolution which may be achieved at longer wavelengths.

With the intensities available, the use of λ ≥ 1.1 Å may be advantageous on other second-generation synchrotron sources such as the SRS (Daresbury), LURE (Paris), NSLS (Brookhaven), MAX-II (Lund), SSRL (Stanford), LNLS (Campinas).

We thank John Helliwell, Sasha Popov and Gleb Bourenkov for helpful suggestions and comments on the manuscript. The financial support from FAPESP and CNPq is acknowledged.

References

Amemiya, Y., Matsushita, T., Nakagawa, A., Satow, Y., Miyahara, J. & Chikawa, J. (1988). *Nucl. Instrum. Methods A*, **266**, 645–653.

Gonzalez, A., Denny, R. & Nave, C. (1994). *Acta Cryst.* D**50**, 276–282.

Helliwell, J. R. (1992). *Macromolecular Crystallography with Synchrotron Radiation.* Cambridge University Press.

Helliwell, J. R. (1993). *Data Collection and Processing*, edited by L. Sawyer, N. Isaacs & S. Bailey, pp. 80–88. Warrington: Daresbury Laboratory.

Helliwell, J. R. (1997). *Methods Enzymol.* **276**, 203–217.

Obmolova, G., Badet-Denisot, M.-A., Badet, B. & Teplyakov, A. (1994). *J. Mol. Biol.* **242**, 703–705.

Otwinowski, Z. (1993). *Data Collection and Processing*, edited by L. Sawyer, N. Isaacs & S. Bailey, pp. 56–62. Warrington: Daresbury Laboratory.

Polikarpov, I., Teplyakov, A. & Oliva, G. (1997). *Acta Cryst.* D**53**, 734–737.